

AERODYNAMIC EFFICIENCY OF GLIDING VEHICLES

Fred Hermanspann, Seattle, USA

Presented at the XXII OSTIV Congress, Uvalde, Texas, USA (1991)

Otto Lilienthal - The Beginning

One hundred years ago Otto Lilienthal fulfilled a lifelong dream and became the first to successfully fly a glider in a repeatable, controlled and documented way, see Figure 1. He is today recognized not only as a courageous and skillful pilot but also as a careful and observant flight test engineer, as an innovative designer, as a tireless visionary who promoted gliding as a sport and even as the first manufacturer of a production glider. One should not forget Lilienthal's scientific achievements, in particular his work that is summarized in his book *Bird Flight as the Basis of Flying*, published in 1889, see Reference 1. Helped by his brother Gustav, he combined careful observations of bird flight with systematic measurements and analysis of model test wings into a theory of aerodynamics that formed the basis for his flying experiments.

In tests of model wings on rotating rigs, the lift and drag forces were referenced to the drag of flat plates at right angles to wind, see Figure 2. By systematic comparison tests, Lilienthal determined that a properly cambered section is much superior to a flat plate in terms of maximum lift and

drag efficiency. He attributed this, without the help of any flow visualization, to its ability to turn the air flow at higher angles without producing "eddies". He correlated this "eddy producing" mechanism also with the rushing noise produced by the different wings at different angles, a first reference to aerodynamic noise. He used the same reasoning - correlating lift with downwash and drag with noise - to postulate that for a given wing area a larger wing span would reduce the "eddy producing" flow around the tips and he even predicted that for a given span a planform with pointed tips would be the most efficient. Aerodynamic theory and airplane design have come a long way since O.

Lilienthal but the search for the most efficient wing sections and planforms is still continuing. The Development of the Sailplane

Despite the success of Lilienthal's experiments - and those of Pilcher, Chanute and the Wrights - no serious glider development took place until after W.W.I. Then, in the early 20's, a loose association of enthusiastic and idealistic students started the modern soaring movement on the Wasserkuppe. In 1921, the first modern "sailplane" appeared, the "Vampyr". It

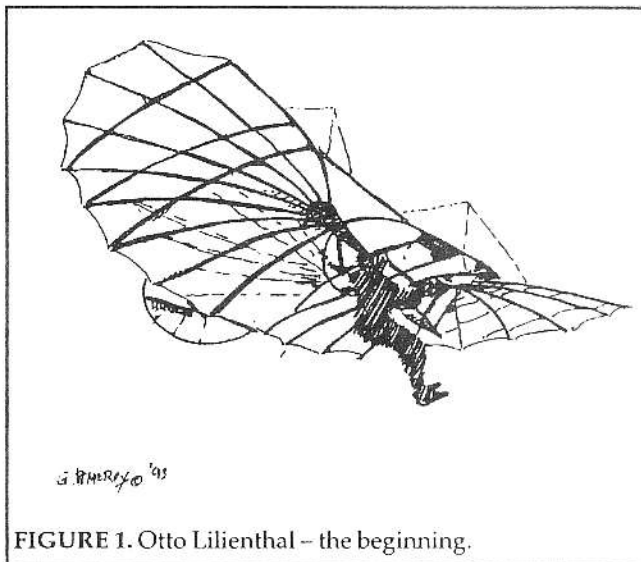
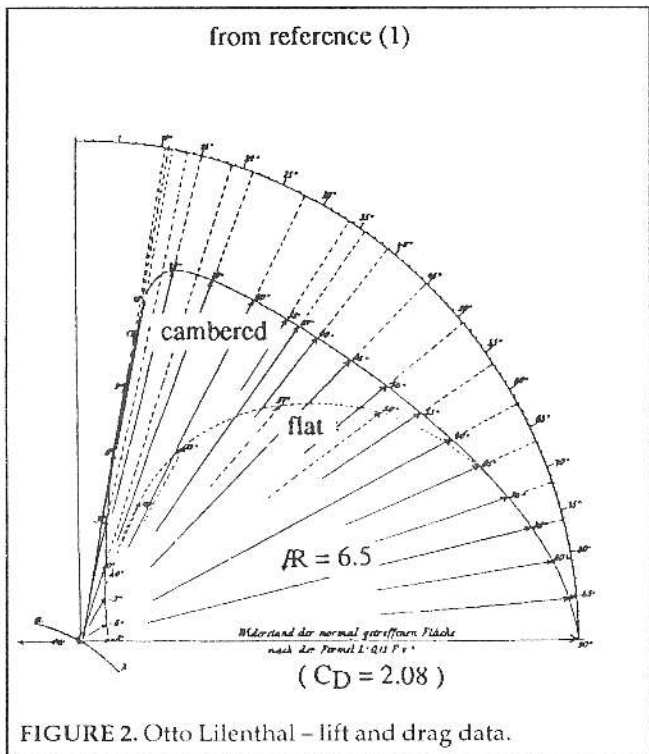
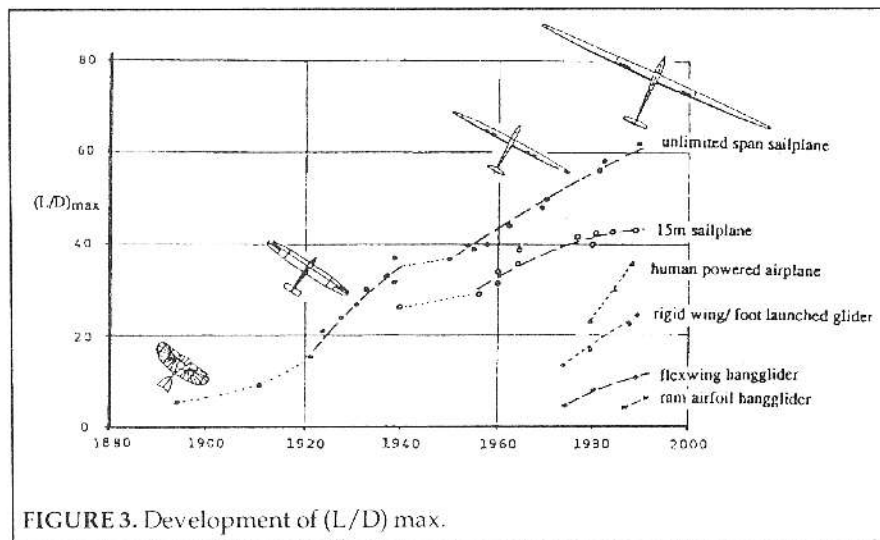


FIGURE 1. Otto Lilienthal - the beginning.



was the first to achieve low sink rates, not by low wing loading, but by improved aerodynamic efficiency. It featured cantilevered wings of relatively high aspect ratio and a streamlined fuselage. Despite a much higher wing loading, it outperformed all competing designs and quickly set the trend for the modern sailplane. Aerodynamic performance – best expressed as the best glide ratio or the $(L/D)_{max}$ (maximum lift/drag ratio) – has improved rapidly ever since, see Figure 3. The wood and canvas designs of the 1930s exceeded already an $(L/D)_{max}$ of 30 and today's composite construction, high-aspect ratio super sailplanes are pushing twice that value, see References 2 to 4. Such performance is unheard of for all other classes of airplanes and has kept



sailplane design in the forefront of aerodynamic and structural development.

Drag Polars and Speed Polars

In nondimensional form, the glide ratio L/D is equal to C_L/C_D , the ratio of lift coefficient to drag coefficient. For conventional configurations the drag coefficient can be approximated by a quadratic function over the usable range of angle of attack – the sum of a constant amount C_{D0} and a term that increases with the square of the lift coefficient, see References 5 and 6:

$$C_D = C_{D0} + k C_L^2 \quad (1)$$

This formula is subject to attached flow and is therefore limited to a certain angle-of-attack range. $(L/D)_{max}$ (MLD) occurs when the constant drag contribution equals the lift dependent drag contributions, i.e. for

$$C_L = \sqrt{C_{D0}/k}$$

with $V_{MLD} = \sqrt{(W/S)/((\rho/2)\sqrt{(C_{D0}/k)})}$
 and $(L/D)_{max} = .5/\sqrt{(C_{D0}/k)}$ (2)
 (W/S wing loading, ρ air density)

This quadratic drag polar can be converted into a speed polar in which the sink rate V_s in steady straight flight is calculated as a function of the forward speed V . This is how gliding performance has been traditionally established. By using normalized speeds, in which the sink rates and forward speeds are referenced to their values at $(L/D)_{max}$, the effects of wing loading and air density can be eliminated, resulting in a normalized speed polar of the form

$$\bar{V}_s = (\bar{V}^3 + 1/\bar{V})/2$$

with $\bar{V} = V/V_{MLD}$
 and $\bar{V}_s = V_s/V_{sMLD}$ (3)

This normalized speed polar is depicted in Figure 4 which also shows the measured speed polars of the Vampyr and of the Nimbus 3, representative of over 60 years of sailplane development. Both follow clearly the idealized shape, but fall significantly short of the minimum sink potential, obviously because of increasing flow separations near stall.

Lift Induced Drag

Lilienthal's deductions about lift-related tip losses, effects of aspect ratio and of planform, were pretty much borne out by Prandtl's lifting line theory and elliptic span loading has long been established as the optimum for minimum induced drag of planar wings (Reference 7). It has also long been known that spreading the trailing vortices vertically can reduce induced drag further. Vertical winglets (see Reference 8) at the tips of a planar wing can reduce induced drag rela-

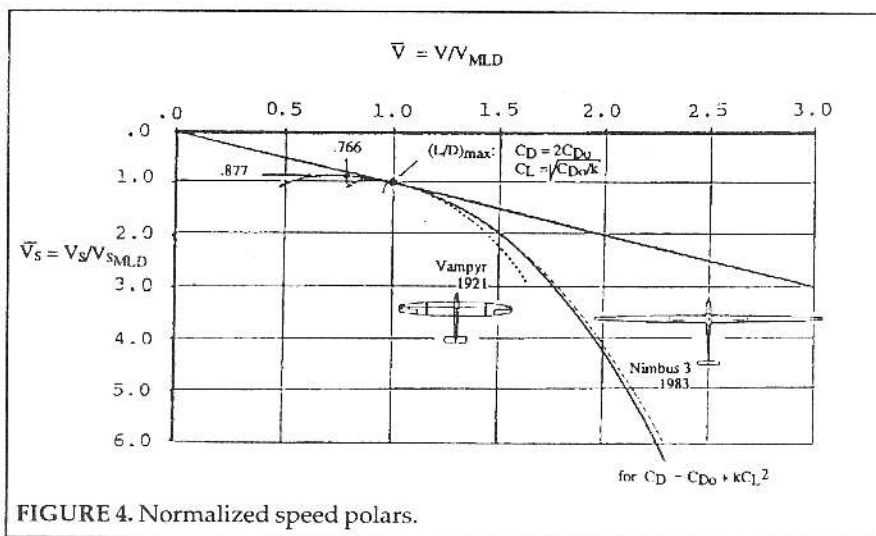


FIGURE 4. Normalized speed polars.

tive to an elliptically loaded planar wing of the same span by about the same amount as a biplane layout of the same span and same vertical spread and are now widely utilized. The induced drag constitutes the quadratic term of the quadratic drag polar (ignoring minor contributions from flow misalignment, Reynolds number changes, etc.).

Friction Drag Contribution

For clean, streamlined shapes such as used on sailplanes skin friction over the exposed surfaces is the only constant (i.e. lift independent) drag contribution. This skin friction—the resistance created by viscous effects on surfaces exposed to a fluid has been scientifically treated since the days of Froude and is commonly referenced to the skin friction of perfect flat plates without pressure gradients or superelevicity. These viscous effects are limited to a thin layer over the exposed surface (“wetted surface”)—Prandtl’s boundary layer. While this boundary layer is normally turbulent, i.e. full of small, random vortices, a special form of the boundary layer exists characterized by smooth, almost stratified flow—the laminar boundary layer. This laminar boundary layer creates significantly lower skin friction, but is also much more sensitive to surface imperfections and adverse pressure gradients. Sailplanes have been using natural laminar flow over part of the exposed surfaces since the mid-1940’s.

The measured minimum drag coefficients (at low to medium lift coefficients) of a number of interesting wing airfoils (from References 9 to 13) indicate that these airfoils indeed achieve substantial laminar boundary layer flow (up to 70% averaged for upper and lower surfaces) up to over $RN = 10^7$.

All these considerations, so far, assume perfect smooth surfaces. However, actual configurations have numerous surface imperfections that can cause early transition and additional roughness drag. Such imperfections range from distributed roughness to individual discontinuities (from doors, controls, etc.), and roughness created by

insects and rain. On a more positive note, recent research (Reference 14) has shown that small streamwise grooves can reduce turbulent skin friction below that for smooth surfaces—indication that the traditional skin friction laws are still subject to change.

In summary, if drag due to flow separation and due to interference can be eliminated, the constant (parasite or zero lift) drag can be determined by the sum of skin friction over the exposed (“wetted”) areas.

Maximum L/D Potential

Combination of the above described parasite and induced drag contributions yields the minimum drag achievable within the configuration parameters of effective aspect ratio, surface areas and skin friction.

eters of effective aspect ratio, surface areas and skin friction.

$$C_D = \Sigma(C_f A/S) + C_L^2 / (\pi AR) \quad (4)$$

(A exposed areas of components)

This equation is basically a more detailed version of Equation 1. If the exposed areas for the individual components (wing, tail surfaces, etc.) are adjusted to a standard reference skin friction coefficient of $C_f = .002$ (Reference 14) this leads to a new expression for $(L/D)_{max}$ as a function of adjusted area ratio and effective aspect ratio:

$$(L/D)_{max} = 19.817 \sqrt{AR'(A/S)'} \quad (5a)$$

with $A' = \Sigma A (C_f/.002)$
adjusted total wetted area
and $AR' = AR$ effective aspect ratio

or

$$(L/D)_{max} = 19.817 b' / \sqrt{(A')} \quad (5b)$$

with $b' = b e$ effective span

This expression can be regarded as representing 100% efficiency for the given parameters and serve as an evaluation tool for the aerodynamic quality of any configuration.

Key Performance Parameters

The key parameters defining the aerodynamic potential in Equation 5 are:

- aspect ratio (R);
- wetted area ratio (A/S); and
- extent of laminar flow (x/c).

These three parameters are nondimensional and geometric; they are also descriptive and indicate graphically the aerodynamic and structural quality built into a configuration. A historical survey of these three parameters for sailplanes is presented in Figure 5. It reflects the evolutionary drive to improve the aerodynamic efficiency and complements the actual $(L/D)_{max}$ data shown

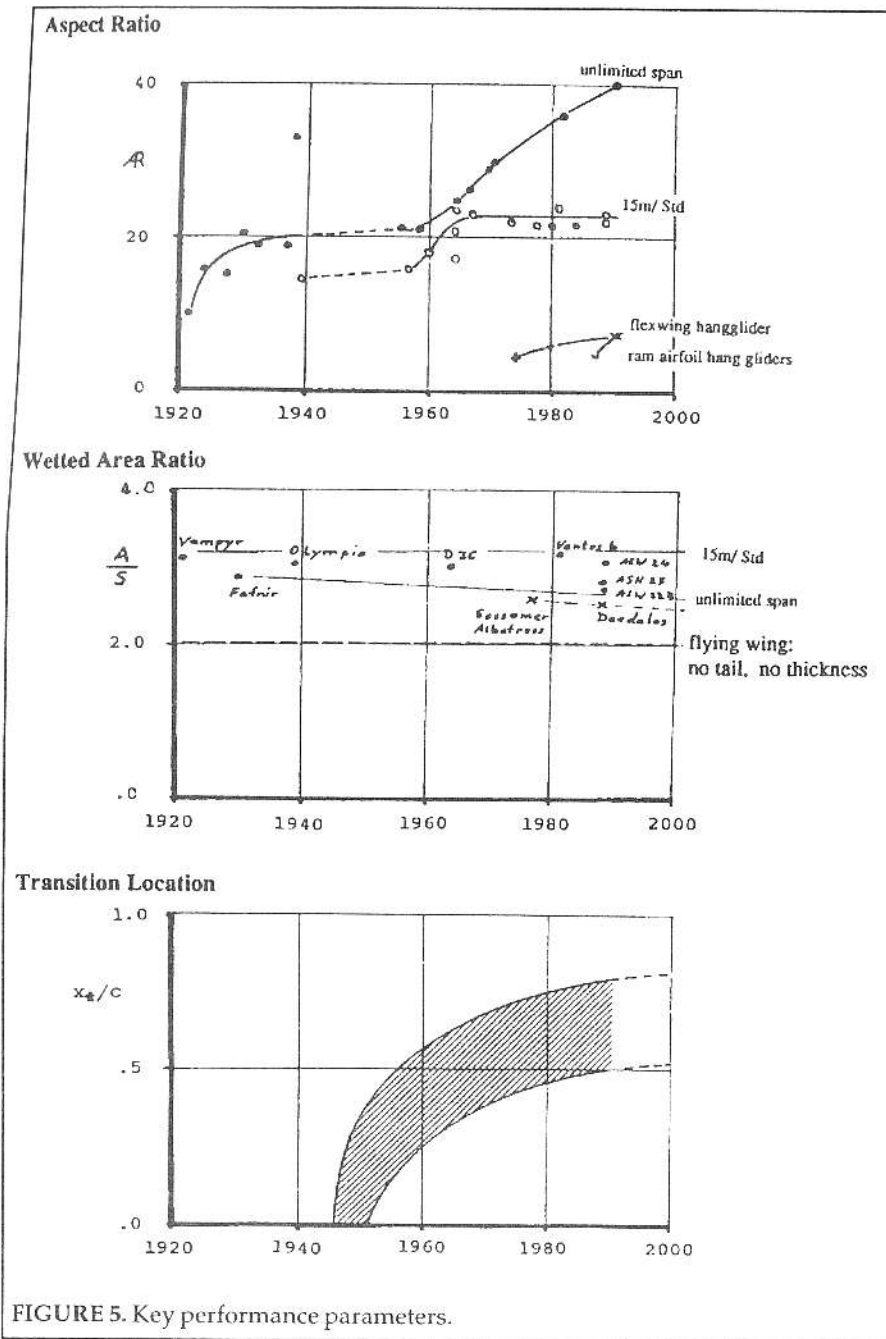


FIGURE 5. Key performance parameters.

in Figure 3.

A high aspect ratio has always been the most visible indication for the aerodynamic quality of a sailplane. It is limited by structural efficiency – i.e. providing adequate strength at acceptable weight – and by constraints stemming from flutter, etc. Realized aspect ratios with wooden designs reached up to 20, while modern composite sailplanes nearly double that value – a remarkable achievement.

The wetted area ratio – the ratio of exposed surface area to wing area – would ideally only represent upper and lower wing surface. Conventional configurations require tail surfaces and a body with wetted area ratios of 2.5 to 3 determine currently the $(L/D)_{max}$ potential. It

is unlikely that cockpit space requirements can be further reduced and – considering human factors and crash-worthiness requirements – they might actually increase. Therefore, further reductions in wetted area ratio will be increasingly difficult.

The boundary layer transition denotes the extent of laminar flow on a surface which characterizes the level of skin friction. Use of natural laminar flow (NLF) airfoils has made great progress. Today's airfoils can provide over 80% laminar flow (lower wing surfaces) at $Re = 10^6$ and further improvements are still possible. This NLF airfoil technology is now increasingly applied to bigger and faster (thus higher Re) airplanes and the soaring community can take pride in having been a major contributor in this development.

Development of Aerodynamic Efficiency

Once the above explained geometry related parameters are established for a particular configuration, the potential $(L/D)_{max}$ can be calculated with Equation 5. Evaluating the actual performance against the theoretical limit provides then the true measure of aerodynamic quality or efficiency. Figure 6 shows to what extent various gliding vehicles have realized their performance potential. The development of the sailplane in particular illustrates the steady improvement in aerodynamic efficiency. From Lilienthal's No. 11 design (1895) with less than 40% to the Vampyr (1921) with about 70%, to the designs of the 1930's with over 90% there was a dramatic improvement due to continuous smoothing and streamlining.

Further configuration cleanups and detail refinements have brought this aerodynamic efficiency up to over 97% on modern competition sailplanes. The modern competition sailplane has thus virtually reached its performance potential for given effective aspect ratio and adjusted wetted area ratio and further performance increases depend on improving these parameters.

Outlook

What performance gains can be expected for the future? Evolutionary refinements in effective aspect ratio, area ratio and particularly laminar flow extent will continue to drive the performance higher, perhaps for unlimited class sailplanes to maximum L/D ratios of over 80.

However, predictions that are based on the past are

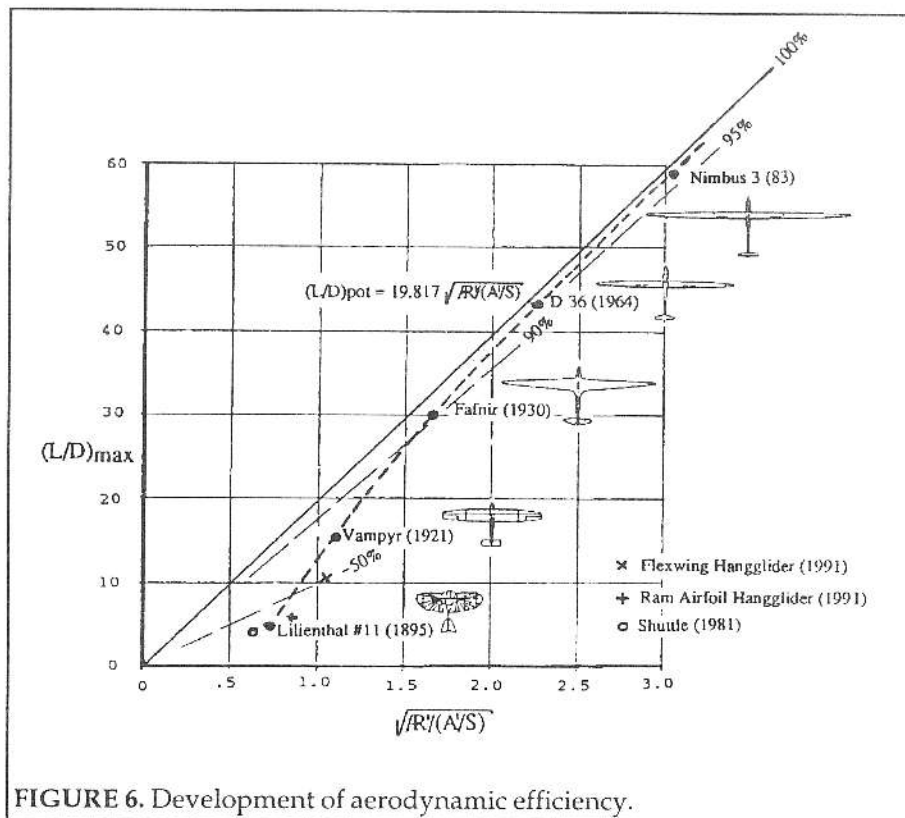


FIGURE 6. Development of aerodynamic efficiency.

always fraught with difficulties and usually serve only to demonstrate the limitations of extrapolation. Just as Otto Lilienthal could not have foreseen the tremendous technical progress in the last 100 years and would have been utterly amazed about what happened to his fragile gliding machine, we cannot possibly imagine all the wonderful and exciting developments in gliding machines by the year 2091!

References

- (1) O. Lilienthal, Birdflight as the Basis of Aviation, 1889.
- (2) J. A. Simpson, The Evolution of the Sailplane, *Soaring*, March/April 1946.
- (3) H. Zacher, 60 Years Akaflieg Darmstadt, *Aerokurier*, January 1981.
- (4) R. H. Johnson, A Flight Evaluation of the Nimbus 3, *Soaring*, December 1982.
- (5) F. Thomas, *Basics of Sailplane Design*, 1984.
- (6) S. Hoerner, *Fluid-Dynamic Drag*, 1965.
- (7) M. M. Munk, *The Minimum Induced Drag of Airfoils*, 1921.
- (8) M. V. Lawson, Minimum Drag for Wings with Spanwise Camber, *J. o. A.*, July 1990.
- (9) W. Feifel, Effects of Reynolds Number on Airfoil Section, NW Soaring Symposium 1974.
- (10) I. H. Abbotts and A. E. Doenhoff, *Theory of Wing Sections*, 1958.
- (11) L. M. M. Boermans and D. C. Terleth, Wind Tunnel Tests of an Airfoil with an Application to the ASW-19B, ICAS-82-5.5.2, 1982.
- (12) D. M. Somers, Design and Experimental Results for a Flapped Natural Laminar Flow Airfoil for General Aviation Applications, NASA IP-11865, 1981.
- (13) D. Althaus, *Stullgarter Profilkatalog I*, 1972.
- (14) W. D. Harvey, Boundary Layer Control for Drag Reduction, AIAA 87-2434, 1984.